A Compact Model of Nanoscale Ferroelectric Capacitor

Chien-Ting Tung, *Graduate Student Member, IEEE*, Girish Pahwa, *Member, IEEE*, Sayeef Salahuddin, *Fellow, IEEE*, and Chenming Hu, *Life Fellow, IEEE*

***Abstract*— In this brief, we present a compact model of nanoscale ferroelectric (FE) capacitors. We first use the phase-field simulation to study the polarization switching of very small FE capacitor that contains only a few grains. We show that at higher applied voltage, the entire grain undergoes a single-domain-like switching, but at lower applied voltage, the domain wall growth mechanism dominates due to the difference between the domain wall energies of bulk and defect nuclei. To create a compact model that includes this voltage dependence, we use a time-dependent domain switching model for each discrete grain with empirical modifications capturing the two different switching mechanisms. In addition, a voltage-dependent dielectric model is included to represent the nonlinear capacitance of the FE capacitor. We verify this compact model by fitting the results of phase-field modeling results with excellent agreement.**

***Index Terms*— Compact model, ferroelectric (FE), hafnium zirconate (HZO), phase-field modeling.**

I. Introduction

THE ferroelectricity of thin-film HfO_2 was discovered in 2011 [1]. Due to its compatibility with the standard CMOS technology, hafnium zirconate (HZO)-based ferroelectric (FE) memories become great candidates for future nonvolatile memory (NVM) applications, such as ferroelectric FET (FEFET), ferroelectric RAM (FERAM), and ferroelectric tunnel junction (FTJ) [2]. The polycrystalline nature of HZO provides the opportunity for multistate operation on FE memories, which can be used on neuromorphic applications [3]. It is the multigrain switching behavior to generate the continuous polarization states. Various experiments and modeling works have been done to study the switching behavior of FE devices [4]–[7] using the nucleation-limited switching (NLS) model with a statistically distributed switching rate. However, when the device area becomes very small, we can no longer describe it with a continuous distribution function. A nanoscale FE capacitor only contains a few grains, which leads to a discrete polarization switching [8], [9]. The NLS model also assumes that the switching is dominated by nucleation due to the small size of the grains. The effect of domain propagation might be therefore averaged out by the statistical distribution of large number of grains in a large-area capacitor. However, it cannot be neglected in case of a small-area capacitor, where there are only a few grains present. As the technology becomes more mature, this kind of nanoscale FE capacitor will be introduced into high-density integrated circuits (ICs). It is essential for us to study its characteristics and have a SPICE-compatible compact model for IC simulation.

Due to the lack of experimental data and the difficulty of measuring polarization-voltage characteristics of such small devices, we need to rely on numerical simulation to study the device. Phase-field modeling using time-dependent Ginzburg Landau (TDGL) theory is the most common way to study FE devices [10]–[13]. In this work, we study the properties of small-area FE by performing the phase-field simulations of FE capacitors with grain size within 20 nm [9], [14]. We then develop a compact model to capture the electrical characteristics resulting from the TDGL model.

II. Phase-Field Simulation

To simulate the nanoscale FE, we conduct a 2-D phase-field simulation using COMSOL Multiphysics [15]. First, we study the switching under a single-grain FE capacitor with 20 nm width and 5 nm thickness. Voltage is applied on the top and bottom boundaries. We set remanent polarization $P_R = 22\ \mu C/cm^2$ and coercive field $E_C = 2$ MV/cm^2 [16]. Inside the capacitor, we add a 1 nm $\times$ 1 nm nucleus, which has an E_C smaller than the bulk value [11] shown in Fig. 1. Here, we set it to be $0.7E_C$ of bulk. The coupled Poisson-TDGL simulation is set as (1), where V is the electrical potential, P_j is the polarization component in the j-direction where $j = x$ or y, ε_r is the relative permittivity (=31), ε_0 is the vacuum permittivity, ρ is the viscosity coefficient (=6 Ωm), α, β, and γ are the Landau–Khalatnikov (LK) coefficients [17], and g is the polarization gradient coefficient (=1e-10 m^3/F). For simplicity, we assume a dielectric relation in the x-direction since, in this study, there is no voltage applied in that direction. We apply $\vec{\nabla} P \cdot \vec{n} = 0$ for every grain boundary where $\vec{n}$ is the

Manuscript received 2 April 2022; revised 21 May 2022; accepted 6 June 2022. Date of publication 16 June 2022; date of current version 25 July 2022. This work was supported by the Berkeley Device Modeling Center, University of California at Berkeley, Berkeley, CA, USA. The review of this article was arranged by Editor A. J. Scholten. *(Corresponding author: Chien-Ting Tung.)*

The authors are with the Department of Electrical Engineering and Computer Sciences, University of California at Berkeley, Berkeley, CA 94720 USA (e-mail: cttung@berkeley.edu).

Color versions of one or more figures in this article are available at https://doi.org/10.1109/TED.2022.3181573.

Digital Object Identifier 10.1109/TED.2022.3181573

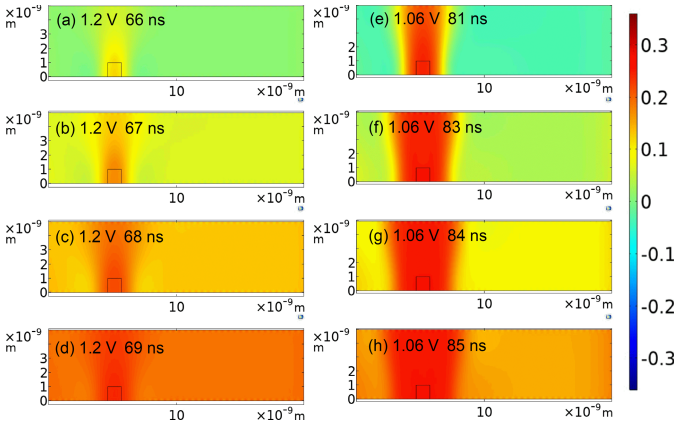

Fig. 1. Polarization switching of a single-grain FE capacitor at 1.2 and 1.06 V. The legend shows the polarization in the unit of C/m^2.

normal vector [18]

$$\vec{\nabla} \cdot (-(\varepsilon_r - 1)\varepsilon_0 \vec{\nabla} V + P) = 0 \tag{1a}$$

$$0 = -(\varepsilon_r - 1)\varepsilon_0 \frac{\partial V}{\partial x} - P_x \tag{1b}$$

$$\rho \frac{\partial P_y}{\partial t} = -\frac{\partial V}{\partial y} - 2\alpha P_y - 4\beta P_y^3 - 6\gamma P_y^5 + 2g\nabla^2 P_y. \tag{1c}$$

Fig. 1 shows the simulation results of this FE capacitor for 1.2 and 1.06 V, respectively. We plot P_y of the entire capacitor at different simulation time instants. We can see that the polarization begins to switch at the nucleus followed by the bulk at 1.2 V. It is similar to single-domain switching since the electric field is strong enough to make nucleus and bulk switch almost at the same time. For 1.06 V, since the applied voltage is close to E_C of the bulk, the bulk will switch much slower than nucleus. The domain propagation can be clearly seen in this case. It becomes a combination of domain wall switching and bulk switching. This phenomenon might be averaged out when there are a lot of grains with different size and material properties.

We also study the case where the device contains three grains in the width direction. Each grain width is set to be 16 nm [14]. We choose three-grain because the dimensions of a short-channel transistor for the state-of-the-art technologies are typically around 20 nm × 50 nm. Given the typical size of grain in HZO is 16–20nm, we think that a three-grain scenario is good enough to study these devices. For example, in [9], a three-grain switching behavior was recently observed for a short-channel FEFET. At the grain boundary, we assume that there is a 0.5-nm dielectric dead layer [19], [20] that will stop the domain propagation. Moreover, in polycrystalline FE, each grain can have different FE properties [5]. Here, for simplicity, we set these grains to have different E_C values, which are 1.7, 2.55, and 2 MV/cm, so that it can perform the discrete switching seen in [9]. Inside each grain, we also place a nucleus the same as the one grain case. Fig. 2 shows that each grain will switch at different times since they have different domain energies.

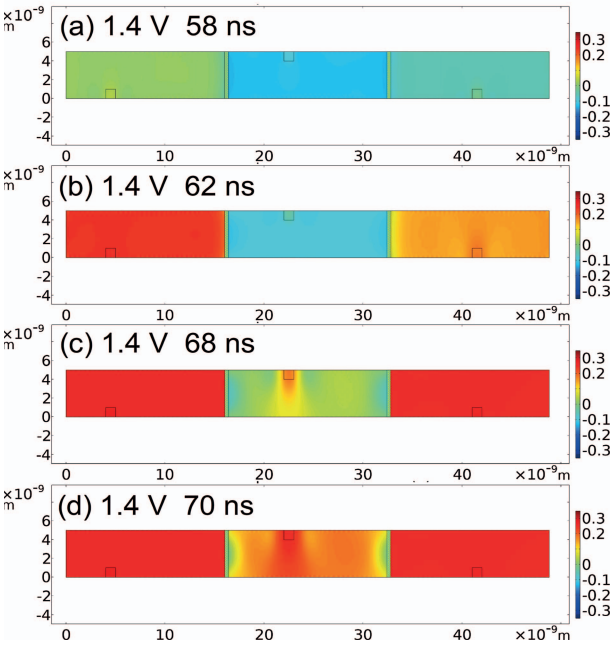

Fig. 2. Polarization switching of a three-grain FE capacitor at 1.4 V. The legends show the polarization in the unit of C/m^2.

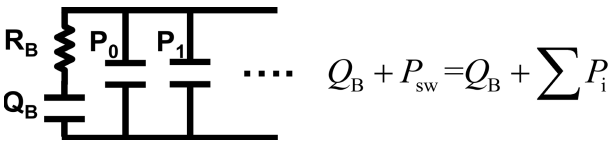

Fig. 3. Equivalent circuit of our nanoscale FE capacitor compact model.

III. Compact Model

We now develop a compact model for nanoscale FE capacitors based on the phase-field simulation results. From Figs. 1 and 2, we can see that due to the nuclei and multi-grains, a single-domain LK equation is not able to describe the system. Depending on the computational penalty, directly coding phase-field model with Verilog-A code is not suitable for a compact model [12]. Therefore, we decide to adopt the domain switching models, such as Kolmogorov–Avrami–Ishibashi (KAI) model and NLS model [7], [21], [22]. We previously developed a compact model for large-area FE capacitor based on these models [6]. We use the same framework to develop a unified compact model valid for both the large- and small-area capacitors.

In this compact model, the FE capacitor is described as a parallel combination of many small FE capacitors each representing a grain, as shown in Fig. 3. As stated earlier, the switching mechanism turns from homogeneous switching to domain nucleation and growth switching when the applied voltage decreases. To model this complex switching mechanism, we use (2)–(4) [6], where the subscript i means the index of the grain, which starts from 1, P_i is the polarization of each grain, η is the fraction of the polarization of each grain to the entire capacitor, τ_i is a time constant following

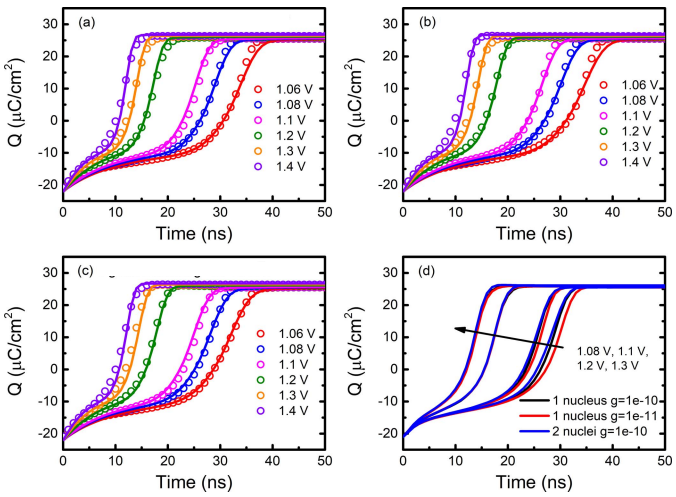

Fig. 4. Model fitting of the single-grain FE capacitors under three cases. (a) One grain one nucleus g = 1e-10 m^3/F. (b) One grain one nucleus g = 1e-11 m^3/F. (c) One grain two nuclei g = 1e-10 m^3/F. The symbols are the COMSOL simulation, and the lines are the compact model. (d) Comparison between three cases.

Merz's law [23], τ_{0i} is the characteristic time constant, E_{ai} is the activation field, t_k is when the electric field changes polarity, and α_i and β_i are the fitting parameters. To capture these two switching behaviors for low and high voltages, we make α_i voltage dependent as (5) with empirical fitting parameters (α_{0i}, δ_i, γ_i, and V_{0i}). α_i will affect the rising time and the spacing between the switching curves at different voltages (see Fig. 4). Therefore, α_i value varies from high-voltage to low-voltage conditions. Since there are only a few grains, we can no longer use a distribution function to describe the grain variation

$$\frac{dP_i}{dt} = \frac{-P_i + \eta_i P_R}{\tau_i(t)}, \quad \text{if } E_{FE}(t) \geq 0$$
$$= \frac{-P_i - \eta_i P_R}{\tau_i(t)}, \quad \text{if } E_{FE}(t) < 0 \tag{2}$$

$$\tau_i(t) = \tau_{0i} \exp\left(\left(\frac{E_{ai}}{|E_{FE}(t)|}\right)^{\alpha_i}\right) \tag{3}$$

$$P_i(t) = \eta_i P_R - (\eta_i P_R - P_i(t_k)) \exp\left(-\left(\int_{t_k}^{t} \frac{1}{\tau_i(t')} dt'\right)^{\beta_i}\right)$$
$$\text{if } E_{FE}(t) \geq 0$$
$$= -\eta_i P_R + (\eta_i P_R + P_i(t_k)) \exp\left(-\left(\int_{t_k}^{t} \frac{1}{\tau_i(t')} dt'\right)^{\beta_i}\right)$$
$$\text{if } E_{FE}(t) < 0 \tag{4}$$

$$\alpha_i(V_{FE}) = \alpha_{0i} - \delta_i \tanh(\gamma_i(V_{FE} - V_{0i})) \tag{5}$$

$$Q_B(V_{FE}) = \frac{\varepsilon_{FE0}}{t_{FE}}\left(V_{FE} + \frac{a V_{FE}}{1 + b(V_{FE} + c \tanh(d P_{sw}))^2}\right). \tag{6}$$

Fig. 4 shows our fitting results compared to phase-field simulation for three different cases: one nucleus with g = 1e-10 m^3/F, one nucleus with g = 1e-11 m^3/F, and two nuclei with g = 1e-10 m^3/F. We can see that the polarization first rises slowly because of the background dielectric response, which is not included in the NLS and KAI models. To capture that, we use the same equations (2)–(4) (with the subscript $i = 0$) and include the background dielectric charge Q_B as in (6) in this model in series with a resistance R_B, where t_{FE} is the FE thickness. Q_B is expressed as a nonlinear function of V_{FE} to model the nonlinearity in the background capacitance, where ε_{FE0} is the nominal permittivity, and a, b, c, and d are the fitting parameters. The total charge is calculated as $Q_B + P_{sw}$, where $P_{sw} = \sum P_i$, which is shown as an equivalent circuit in Fig. 3. This model can capture the switching under different voltages for the three cases shown in Fig. 4. We can also see that the larger the g and number of nuclei, faster is the switching especially when the voltage is low.

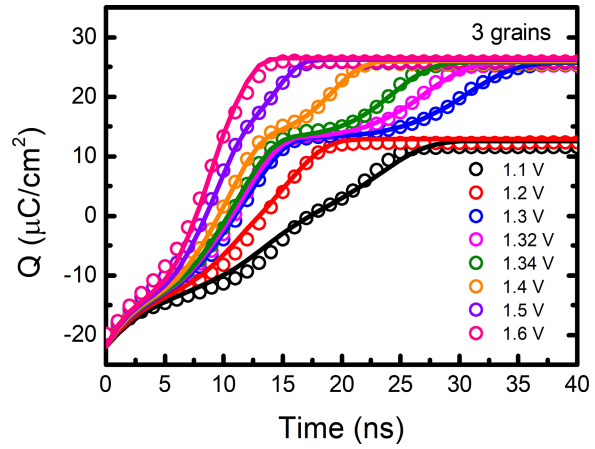

Fig. 5. Model fitting of the three-grain FE capacitor.

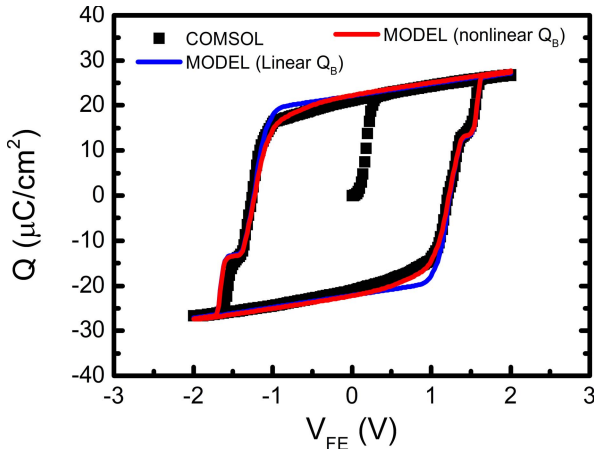

Fig. 6. Comparison between the COMSOL simulated P–V curve and the compact model simulations using linear Q_B and nonlinear Q_B.

Now, we move on to the three grains case. Since we choose a large E_C variation in our simulation, we need to use i = 0, 1, 2, and 3 to fit the data. The result is shown in Fig. 5. The discrete switching comes from the E_C variation of each grain. By selecting different parameters of each P_i, the model can fit the phase-field simulation well. Then, we simulate a P–V loop with a 2.5-MHz triangular voltage wave, as shown in Fig. 6. It shows (6) can fit the nonlinear background capacitance behavior well as compared to the linear charge model. The result shows a good agreement to the COMSOL simulation.

To summarize the difference between the proposed small FE capacitor model and the previous large FE capacitor

model [6], first, the grain distribution is considered discrete instead of continuous due to the small number of the grains; second, we include the nonlinear effect in the background dielectric rather than using a linear background capacitance; third, we modify the switching rate of this model to account for the different switching behaviors at low voltages and high voltages.

IV. Conclusion

We have analyzed the switching behavior of very small FE capacitors that contain a few FE crystal grains using phase-field simulation. The results show that at higher voltage, the switching mechanism is almost single-domain switching and, at lower voltage, it is a combination of domain wall switching and bulk spontaneous switching. We use these results to develop a compact model based on our previous large-area FE capacitor model. This model can simulate the change in the switching mechanism of nanoscale FE capacitor at all voltages including the discrete switching of different grains and the nonlinear capacitance of the FE material.

References

[1] T. S. Böscke, J. Müller, D. Bräuhaus, U. Schröder, and U. Böttger, "Ferroelectricity in hafnium oxide thin films," *Appl. Phys. Lett.*, vol. 99, no. 10, Sep. 2011, Art. no. 102903, doi: 10.1063/1.3634052.

[2] A. Keshavarzi, K. Ni, W. Van Den Hoek, S. Datta, and A. Raychowdhury, "Ferroelectronics for edge intelligence," *IEEE Micro*, vol. 40, no. 6, pp. 33–48, Nov./Dec. 2020, doi: 10.1109/MM.2020.3026667.

[3] E. W. Kinder, C. Alessandri, P. Pandey, G. Karbasian, S. Salahuddin, and A. Seabaugh, "Partial switching of ferroelectrics for synaptic weight storage," in *Proc. 75th Annu. Device Res. Conf. (DRC)*, South Bend, IN, USA, Jun. 2017, pp. 1–2.

[4] C. Alessandri, P. Pandey, A. Abusleme, and A. Seabaugh, "Monte Carlo simulation of switching dynamics in polycrystalline ferroelectric capacitors," *IEEE Trans. Electron Devices*, vol. 66, no. 8, pp. 3527–3534, Aug. 2019, doi: 10.1109/TED.2019.2922268.

[5] C. Alessandri, P. Pandey, A. Abusleme, and A. Seabaugh, "Switching dynamics of ferroelectric Zr-doped HfO_2," *IEEE Electron Device Lett.*, vol. 39, no. 11, pp. 1780–1783, Nov. 2018, doi: 10.1109/LED.2018.2872124.

[6] C. T. Tung, G. Pahwa, S. Salahuddin, and C. Hu, "A compact model of polycrystalline ferroelectric capacitor," *IEEE Trans. Electron Devices*, vol. 68, no. 10, pp. 5311–5314, Oct. 2021, doi: 10.1109/TED.2021.3100814.

[7] A. K. Tagantsev, I. Stolichnov, N. Setter, J. S. Cross, and M. Tsukada, "Non-Kolmogorov–Avrami switching kinetics in ferroelectric thin films," *Phys. Rev. B, Condens. Matter*, vol. 66, no. 21, Dec. 2002, Art. no. 214109, doi: 10.1103/PhysRevB.66.214109.

[8] H. Mulaosmanovic *et al.*, "Evidence of single domain switching in hafnium oxide based FeFETs: Enabler for multi-level FeFET memory cells," presented at the IEDM Tech. Dig., Washington, DC, USA, Dec. 2015.

[9] H. Mulaosmanovic *et al.*, "Switching kinetics in nanoscale hafnium oxide based ferroelectric field-effect transistors," *ACS Appl. Mater. Interfaces*, vol. 9, no. 4, pp. 3792–3798, Feb. 2017, doi: 10.1021/acsami.6b13866.

[10] A. K. Saha, K. Ni, S. Dutta, S. Datta, and S. Gupta, "Phase field modeling of domain dynamics and polarization accumulation in ferroelectric HZO," *Appl. Phys. Lett.*, vol. 114, no. 20, May 2019, Art. no. 202903, doi: 10.1063/1.5092707.

[11] S. Smith, K. Chatterjee, and S. Salahuddin, "Multidomain phase-field modeling of negative capacitance switching transients," *IEEE Trans. Electron Devices*, vol. 65, no. 1, pp. 295–298, Jan. 2018, doi: 10.1109/TED.2017.2772780.

[12] C.-S. Hsu, S.-C. Chang, D. E. Nikonov, I. A. Young, and A. Naeemi, "A theoretical study of multidomain ferroelectric switching dynamics with a physics-based SPICE circuit model for phase-field simulations," *IEEE Trans. Electron Devices*, vol. 67, no. 7, pp. 2952–2959, Jul. 2020, doi: 10.1109/TED.2020.2990891.

[13] A. K. Saha, M. Si, K. Ni, S. Datta, P. D. Ye, and S. K. Gupta, "Ferroelectric thickness dependent domain interactions in FEFETs for memory and logic: A phase-field model based analysis," in *IEDM Tech. Dig.*, Dec. 2020, pp. 3–4, doi: 10.1109/IEDM13553.2020.9372099.

[14] J. Liao *et al.*, "Grain size engineering of ferroelectric Zr-doped HfO_2 for the highly scaled devices applications," *IEEE Electron Device Lett.*, vol. 40, no. 11, pp. 1868–1871, Nov. 2019, doi: 10.1109/LED.2019.2944491.

[15] *COMSOL Multiphysics V. 5.6*. Accessed: Nov. 1, 2021. [Online]. Available: https://www.comsol.com

[16] M. Si *et al.*, "Ultrafast measurements of polarization switching dynamics on ferroelectric and anti-ferroelectric hafnium zirconium oxide," *Appl. Phys. Lett.*, vol. 115, no. 7, Aug. 2019, Art. no. 072107, doi: 10.1063/1.5098786.

[17] L. D. Landau and I. M. Khalatnikov, "On the anomalous absorption of sound near a second order phase transition point," *Doklady Akademii Nauk SSSR*, vol. 96, pp. 469–472, May 1954.

[18] D. Schrade, R. Mueller, B. X. Xu, and D. Gross, "Domain evolution in ferroelectric materials: A continuum phase field model and finite element implementation," *Comput. Methods Appl. Mech. Eng.*, vol. 196, nos. 41–44, pp. 4365–4374, Sep. 2007, doi: 10.1016/j.cma.2007.05.010.

[19] L. J. Sinnamon, M. M. Saad, R. M. Bowman, and J. M. Gregg, "Exploring grain size as a cause for 'dead-layer' effects in thin film capacitors," *Appl. Phys. Lett.*, vol. 81, no. 4, pp. 703–705, Jul. 2002, doi: 10.1063/1.1494837.

[20] W. Shu, J. Wang, and T.-Y. Zhang, "Effect of grain boundary on the electromechanical response of ferroelectric polycrystals," *J. Appl. Phys.*, vol. 112, no. 6, Sep. 2012, Art. no. 064108, doi: 10.1063/1.4752269.

[21] Y. Ishibashi and Y. Takagi, "Note on ferroelectric domain switching," *J. Phys. Soc. Jpn.*, vol. 31, no. 2, pp. 506–510, Aug. 1971, doi: 10.1143/JPSJ.31.506.

[22] M. Avrami, "Kinetics of phase change. I general theory," *J. Chem. Phys.*, vol. 7, no. 12, pp. 1103–1112, Dec. 1939, doi: 10.1063/1.1750380.

[23] W. J. Merz, "Domain formation and domain wall motions in ferroelectric $BaTiO_3$ single crystals," *Phys. Rev.*, vol. 95, no. 3, pp. 690–698, Aug. 1954, doi: 10.1103/PhysRev.95.690.